



HAL
open science

A Marker-and-Cell scheme for viscoelastic flows on nonuniform grids

Omar Mokhtari, Yohan Davit, Jean-Claude Latché, Romain de Loubens,
Michel Quintard

► **To cite this version:**

Omar Mokhtari, Yohan Davit, Jean-Claude Latché, Romain de Loubens, Michel Quintard. A Marker-and-Cell scheme for viscoelastic flows on nonuniform grids. FVCA 2020: Finite Volumes for Complex Applications IX, Jun 2020, Bergen, Norway. pp.645-653. hal-02950581

HAL Id: hal-02950581

<https://hal.science/hal-02950581>

Submitted on 28 Sep 2020

HAL is a multi-disciplinary open access archive for the deposit and dissemination of scientific research documents, whether they are published or not. The documents may come from teaching and research institutions in France or abroad, or from public or private research centers.

L'archive ouverte pluridisciplinaire **HAL**, est destinée au dépôt et à la diffusion de documents scientifiques de niveau recherche, publiés ou non, émanant des établissements d'enseignement et de recherche français ou étrangers, des laboratoires publics ou privés.



Open Archive Toulouse Archive Ouverte

OATAO is an open access repository that collects the work of Toulouse researchers and makes it freely available over the web where possible

This is an author's version published in: <https://oatao.univ-toulouse.fr/26547>

Official URL :

https://doi.org/10.1007/978-3-030-43651-3_61

To cite this version:

Mokhtari, Omar and Davit, Yohan and Latché, Jean-Claude and de Loubens, Romain and Quintard, Michel *A Marker-and-Cell scheme for viscoelastic flows on nonuniform grids.* (2020) In: FVCA 2020: Finite Volumes for Complex Applications IX, 15 June 2020 - 19 June 2020 (Bergen, Norway).

Any correspondence concerning this service should be sent to the repository administrator: tech-oatao@listes-diff.inp-toulouse.fr

A Marker-and-Cell scheme for viscoelastic flows on nonuniform grids

O. Mokhtari, Y. Davit, J.-C. Latché, R. de Loubens, and M. Quintard

Abstract In this paper, we develop a numerical scheme for the solution of the coupled Stokes and Navier-Stokes equations with constitutive equations describing the flow of viscoelastic fluids. The space discretization is based on the so-called Marker-And-Cell (MAC) scheme. The time discretization uses a fractional-step algorithm where the solution of the Navier-Stokes equations is first obtained by a projection method and then the transport-reaction equation for the conformation tensor is solved by a finite-volume scheme. In order to obtain consistency, the space discretization of the divergence of the elastic part of the stress tensor in the momentum balance equation is derived using a weak form of the MAC scheme. For stability and accuracy reasons, the solution of the transport-reaction equation for the conformation tensor is split into pure convection steps, with a change of variable from \mathbf{c} to $\log(\mathbf{c})$, and a reaction step, which consists in solving one ODE per cell via an Euler scheme with local sub-cycling. Numerical computations for the Stokes flow of an Oldroyd-B fluid in the lid-driven cavity at $We=1$ confirm the scheme efficiency.

Key words: Viscoelastic flows, MAC scheme, projection scheme

Omar Mokhtari - Yohan Davit - Michel Quintard
Institut de Mécanique des Fluides de Toulouse (IMFT), CNRS, Toulouse, France
e-mail: (yohan.davit, omar.mokhtari, michel.quintard)toulouse-inp.fr

Romain de Loubens
Total E&P, CSTJF, Pau, France,
e-mail: romain.de-loubens@total.com

Jean-Claude Latché
Institut de Radioprotection et de Sécurité Nucléaire, Cadarache, France,
e-mail: jean-claude.latche@irsn.fr

1 Introduction

We consider viscoelastic models for polymeric incompressible liquids. Let Ω be a parallelepiped of \mathbb{R}^d , $d \in \{2, 3\}$ and $(0, T)$, $T > 0$, a finite time interval. The fluid is governed by the following system of equations:

$$\rho(\partial_t \mathbf{u} + \xi \mathbf{u} \cdot \nabla \mathbf{u}) = -\nabla p + \operatorname{div} \tau_s(\mathbf{u}) + \operatorname{div} \tau_p, \quad \tau_p = \frac{\eta_p}{\lambda} \mathbf{f}(\mathbf{c})(\mathbf{c} - \mathbf{I}_d), \quad (1a)$$

$$\operatorname{div} \mathbf{u} = 0, \quad (1b)$$

$$\partial_t \mathbf{c} + \mathbf{u} \cdot \nabla \mathbf{c} - (\nabla \mathbf{u}) \mathbf{c} - \mathbf{c} (\nabla \mathbf{u})^t + \frac{1}{\lambda} \mathbf{g}(\mathbf{c})(\mathbf{c} - \mathbf{I}_d) = 0, \quad (1c)$$

where the vector-valued function \mathbf{u} is the velocity of the fluid, p is the pressure, $\tau_s = \eta_s(\nabla \mathbf{u} + (\nabla \mathbf{u})^t)$ is the Newtonian stress tensor for the solvent with η_s its viscosity. The constant coefficients ρ , η_p and λ are the fluid density, the polymer viscosity and the polymer retardation time. The tensor τ_p is the part of the stress accounting for the presence of polymers and \mathbf{c} is the conformation tensor. The coefficient ξ is zero for the unsteady Stokes equations and $\xi = 1$ for the Navier-Stokes equations. The functions $\mathbf{f}(\mathbf{c})$ and $\mathbf{g}(\mathbf{c})$ depend on the model. For example (see [1] for a review), the Oldroyd-B model is given by $\mathbf{f}(\mathbf{c}) = \mathbf{g}(\mathbf{c}) = \mathbf{I}_d$, and the Fene-CR model corresponds to $\mathbf{f}(\mathbf{c}) = \mathbf{g}(\mathbf{c}) = \frac{b}{b - \operatorname{tr}(\mathbf{c})} \mathbf{I}_d$, with b a real number greater than the space dimension. This system must be complemented by initial conditions for the velocity and the conformation tensor, and by suitable boundary conditions. Here, we suppose for short that the velocity is prescribed over the whole boundary and that the normal velocity vanishes everywhere on the boundary. The dimensionless parameters that characterize these types of flows are the Reynolds number, $Re = \rho UL / (\eta_s + \eta_p)$, and the Weissenberg number, $We = \lambda U / L$, where U and L are the characteristic velocity and length scale.

Here, we develop a numerical scheme for the solution of System (1) based on the following technology. The space discretization is based on the so-called Marker-And-Cell (MAC) scheme. Previous work on MAC schemes for viscoelastic flows can be found in [7], in the context of finite differences and in [4], in the context of finite volumes, both on uniform grids. The time discretization uses a fractional-step algorithm where the solution of the Navier-Stokes equations (1a)-(1b) is first obtained by a standard projection method and then the transport-reaction equation for the conformation tensor (1c) is solved by a finite-volume scheme. The development of this scheme faces two essential difficulties. Firstly, we use a weak formulation of (1a) for the discretization of the term $\operatorname{div} \tau_p$, which yields an essential ingredient for the scheme stability and a built-in Lax-Wendroff weak consistency property (see [5]). Secondly, the solution of Equation (1c) requires special care due to the stiffness of the term $(\nabla \mathbf{u}) \mathbf{c} + \mathbf{c} (\nabla \mathbf{u})^t$. In the spirit of [8], the solution procedure for Equation (1c) is split in pure convection steps, with a change of variable from \mathbf{c} to $\log(\mathbf{c})$, and a reaction step, which consists in solving one ODE per cell thanks to the piecewise constant discretization of \mathbf{c} . In contrast with [8], these ODEs are solved directly for \mathbf{c} , and not $\log(\mathbf{c})$, so as to avoid any artificial introduction of nonlinearities. We

further use a local time step for each cell, which ensures the scheme stability and prevents a blow-up of the CPU cost.

2 The numerical scheme

Let \mathcal{M} be a MAC mesh (see [6]) of Ω . The discrete pressure and conformation unknowns are associated with the cells of the mesh \mathcal{M} and are denoted by $\{p_K, K \in \mathcal{M}\}$ and $\{\mathbf{c}_K, K \in \mathcal{M}\}$. \mathcal{E} and \mathcal{E}_{int} are, respectively, the sets of all $(d-1)$ -faces σ of the mesh and of the interior faces (*i.e.* the faces which are not included in the boundary). For $1 \leq i \leq d$, we denote by $\mathcal{E}_{\text{int}}^{(i)}$ the subset of the faces that are perpendicular to the i^{th} unit vector of the canonical basis of \mathbb{R}^d . The discrete velocity unknowns approximate the normal velocity to the mesh faces. Since the velocity is prescribed on the whole boundary, the degrees of freedom for the i^{th} component of the velocity are associated to $\mathcal{E}_{\text{int}}^{(i)}$ and read $(u_{\sigma,i})_{\sigma \in \mathcal{E}_{\text{int}}^{(i)}}$.

Let us consider a uniform partition $0 = t_0 < t_1 < \dots < t_N = T$ of $(0, T)$ with a constant time step δt . The pressure correction scheme consists in the following two steps:

Prediction step – Solve for $\tilde{\mathbf{u}}^{n+1}$:

$$\begin{aligned} \text{For } 1 \leq i \leq d, \forall \sigma \in \mathcal{E}_{\text{int}}^{(i)}, \\ \frac{\rho}{\delta t} \left(\tilde{u}_{\sigma,i}^{n+1} - u_{\sigma,i}^n \right) + \xi \rho \operatorname{div}_{\sigma} (\tilde{u}_i^{n+1} \mathbf{u}^n) - \operatorname{div}_{\sigma,i} \tau_s(\tilde{\mathbf{u}}^{n+1}) \\ - \operatorname{div}_{\sigma,i} \tau_p^n + \nabla_{\sigma,i} (p^n) = 0. \end{aligned} \quad (2a)$$

Correction step – Solve for p^{n+1} and \mathbf{u}^{n+1} :

$$\text{For } 1 \leq i \leq d, \forall \sigma \in \mathcal{E}_{\text{int}}^{(i)}, \quad \frac{\rho}{\delta t} (u_{\sigma,i}^{n+1} - \tilde{u}_{\sigma,i}^{n+1}) + \nabla_{\sigma,i} (p^{n+1} - p^n) = 0, \quad (2b)$$

$$\forall K \in \mathcal{M}, \quad \operatorname{div}_K (\mathbf{u}^{n+1}) = 0. \quad (2c)$$

In the prediction step, the tensor τ_p^n is computed as a function of the conformation tensor by $\tau_{pK}^n = \frac{\eta_{pK}}{\lambda_K} \mathbf{f}(\mathbf{c}_K^n) (\mathbf{c}_K^n - \mathbf{I}_d)$, for $K \in \mathcal{M}$.

The discretization of the constitutive equation (1c) is split into pure advection steps and a local ODE, which is a strategy already adopted in [8]. This allows us to preserve the positivity of \mathbf{c} and obtain good accuracy. Furthermore, we use a change of variables for the advection steps and change the conformation tensor into the matrix logarithm of the conformation tensor [4]. The result is the following ‘‘Strang-log’’ scheme:

Advection I – Solve for $\mathbf{c}^{n+\frac{1}{3}}$:

$$\forall K \in \mathcal{M}, \quad \frac{1}{\delta t/2} \left(\log \mathbf{c}_K^{n+\frac{1}{3}} - \log \mathbf{c}_K^n \right) + \operatorname{div}_K(\mathbf{u}^{n+1} \log \mathbf{c}_K^{n+\frac{1}{3}}) = 0, \quad (3a)$$

ODE – Set $\mathbf{c}_K(t_n) = \mathbf{c}_K^{n+\frac{1}{3}}$ and solve for $\mathbf{c}^{n+\frac{2}{3}} = \mathbf{c}_K(t_n + \delta t)$:

$$\forall K \in \mathcal{M}, \quad \partial_t \mathbf{c}_K - (\nabla_K \mathbf{u}^{n+1}) \mathbf{c}_K - \mathbf{c}_K (\nabla_K \mathbf{u}^{n+1})^t + \frac{1}{\lambda_K} \mathbf{g}(\mathbf{c}_K)(\mathbf{c}_K - \mathbf{I}_d) = 0, \quad (3b)$$

Advection II – Solve for \mathbf{c}^{n+1} :

$$\forall K \in \mathcal{M}, \quad \frac{1}{\delta t/2} \left(\log \mathbf{c}_K^{n+1} - \log \mathbf{c}_K^{n+\frac{2}{3}} \right) + \operatorname{div}_K(\mathbf{u}^{n+1} \log \mathbf{c}_K^{n+1}) = 0. \quad (3c)$$

Transport steps are discretized by a standard first-order upwind scheme. The local ODE (3b) is solved using a first-order Euler scheme, with a local sub-time step. Two versions are tested: the fully implicit scheme and a version where the term $(\nabla_K \mathbf{u}^{n+1}) \mathbf{c}_K + \mathbf{c}_K (\nabla_K \mathbf{u}^{n+1})^t$ is explicit, while the other ones are still implicit. From a theoretical point of view, both variants seem to have the same stability properties, *i.e.* to preserve the positive definite character of the conformation tensor for a small enough (sub-)time step, depending on the velocity gradient. However, numerical tests show that the implicit version is more stable.

Most discrete operators involved in the scheme are standard and we refer to [6] for their detailed definition. We focus in the next section on the discretization of the divergence of the stress tensor in the momentum balance equation.

3 The total stress divergence term

The aim of this section is to define the divergence term $\operatorname{div}_{\sigma,i}(\mathbf{T})$ of the total Cauchy stress tensor $\mathbf{T} = -p\mathbf{I}_d + \tau_s(\tilde{\mathbf{u}}) + \tau_p$. We want this quantity to satisfy a discrete analogue of the identity:

$$\int_{\Omega} \operatorname{div}(\mathbf{T}) \cdot \mathbf{u} = - \int_{\Omega} \mathbf{T}(\mathbf{u}) : \nabla \mathbf{u}. \quad (4)$$

This relation is crucial to derive a scheme that preserves a free energy estimate at the discrete level [2]. In addition, if the discrete gradient of the interpolation of a regular function converges to the continuous gradient in L^∞ -weak \star , which is the case here (with, in fact, a strong L^∞ convergence), then the identity (4) readily yields the Lax-Wendroff consistency of the discretization of the term $\operatorname{div}_{\sigma,i}(\tau_p^n)$. The strategy to obtain (4), already used in [6] for Newtonian fluids, is to recast the MAC scheme under a weak form. For clarity, we only address the two-dimensional case here. The extension to the three-dimensional case is presented in [6].

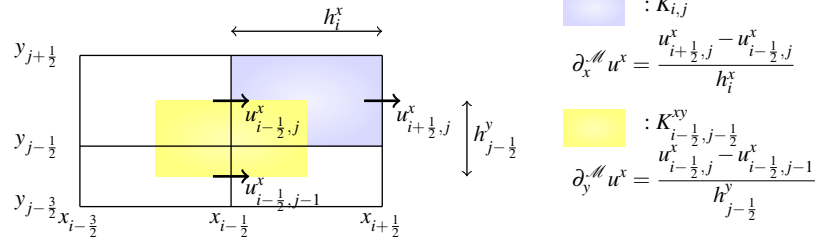


Fig. 1 Discrete partial derivatives of the x -component of the velocity

The discrete velocity gradient – Here, we detail the discretization of terms associated to the x -component of the velocity, using the notations of Fig. 1. Inside the computational domain, the discrete partial derivatives of this velocity component are defined as follows:

- Let the primal cells be denoted by $K_{i,j} = (x_{i-1/2}, x_{i+1/2}) \times (y_{j-1/2}, y_{j+1/2})$. The discrete derivative involved in the divergence (so, for the velocity x -component, only $\partial_x^{\mathcal{M}} u^x$) is defined over the primal cell by, $\forall \mathbf{x} \in K_{i,j}$:

$$\partial_x^{\mathcal{M}} u^x(\mathbf{x}) = \frac{u_{i+1/2,j}^x - u_{i-1/2,j}^x}{h_i^x}. \quad (5)$$

- For the other derivatives (so, for the velocity x -component, only $\partial_y^{\mathcal{M}} u^x$), we introduce a fourth mesh which is vertex-centred, and we denote by K^{xy} the generic cell of this new mesh, with $K_{i-1/2,j-1/2}^{xy} = (x_{i-1}, x_i) \times (y_{j-1}, y_j)$. Then, $\forall \mathbf{x} \in K_{i-1/2,j-1/2}^{xy}$:

$$\partial_y^{\mathcal{M}} u^x(\mathbf{x}) = \frac{u_{i-1/2,j}^x - u_{i-1/2,j-1}^x}{h_{j-1/2}^y}. \quad (6)$$

The only necessary extension of this definition to cope with boundaries concerns the definition of $\partial_y^{\mathcal{M}} u^x$ over a half vertex-centred cell associated with a vertex lying on a horizontal boundary. In this case, we use the usual “fictitious cell trick” in order to apply Relation (6): an external cell, of zero y -dimension, is added to the mesh and the horizontal velocity in this cell is set to the prescribed Dirichlet value, or to zero for the test functions defined below. Extending these definitions to the y -component of the velocity, the discrete diffusion tensor can be defined as:

$$\nabla^{\mathcal{M}} \tilde{\mathbf{u}} = \begin{bmatrix} \partial_x^{\mathcal{M}} \tilde{u}^x & \partial_y^{\mathcal{M}} \tilde{u}^x \\ \partial_x^{\mathcal{M}} \tilde{u}^y & \partial_y^{\mathcal{M}} \tilde{u}^y \end{bmatrix}, \quad \tau^{\mathcal{M}}(\tilde{\mathbf{u}}) = \eta_s \left(\nabla^{\mathcal{M}} \tilde{\mathbf{u}} + (\nabla^{\mathcal{M}} \tilde{\mathbf{u}})^t \right). \quad (7)$$

Finite-volume test functions – Let us denote by $\mathcal{S}^x \subset \mathbb{N}^2$ (resp. $\mathcal{S}^y \subset \mathbb{N}^2$) the set of pairs (i, j) such that $\mathbf{x}_{i-1/2,j}$ (resp. $\mathbf{x}_{i,j-1/2}$) is the mass center of a vertical (resp.

horizontal) face of the mesh. For $(i, j) \in \mathcal{S}^x$, we denote by $\phi^{x,(i-\frac{1}{2},j)}$ the test function associated with the degree of freedom of the x -component of the velocity located at $\mathbf{x}_{i-\frac{1}{2},j}$. This discrete function is defined by:

$$(\phi^{x,(i-\frac{1}{2},j)})_{k-\frac{1}{2},\ell}^x = \delta_k^i \delta_\ell^j, \quad \forall (k, \ell) \in \mathcal{S}^x \text{ and } (\phi^{x,(i-\frac{1}{2},j)})_{k,\ell-\frac{1}{2}}^y = 0, \quad \forall (k, \ell) \in \mathcal{S}^y.$$

Its non-zero partial derivatives are $\partial_x^{\mathcal{M}} \phi^{x,(i-\frac{1}{2},j)}$ and $\partial_y^{\mathcal{M}} \phi^{x,(i-\frac{1}{2},j)}$ and are given by (5) and (6), respectively. Since the velocity is prescribed on the boundary, no equation is written on the half-dual cells associated to external faces, so no definition is required for the corresponding test functions.

Discrete viscous diffusion and pressure gradient – The discrete divergence of the stress tensor for the solvent is defined by the following weak formulation:

$$\forall (i, j) \in \mathcal{S}^x, \quad -(\operatorname{div} \tau_s(\tilde{\mathbf{u}}))_{i-\frac{1}{2},j}^x = \frac{1}{|K_{i-\frac{1}{2},j}^x|} \int_{\Omega} \tau_s^{\mathcal{M}}(\tilde{\mathbf{u}}) : \nabla^{\mathcal{M}} \phi^{x,(i-\frac{1}{2},j)}. \quad (8)$$

Similarly, identifying p with its associated piecewise constant function, we have for the pressure gradient:

$$\forall (i, j) \in \mathcal{S}^x, \quad (\nabla p)_{i-\frac{1}{2},j}^x = \frac{-1}{|K_{i-\frac{1}{2},j}^x|} \int_{\Omega} p \partial_x^{\mathcal{M}} \phi^{x,(i-\frac{1}{2},j)} \quad (9)$$

It is shown in [6] that Equation (8) yields the usual finite-volume formulation of the MAC scheme. The same holds for the definition (9) of the pressure gradient.

Polymeric stress tensor divergence – This formulation naturally extends to the discretization of the divergence of the polymeric stress tensor. To do so, we first associate the discrete polymeric stress τ_p to a piecewise function over the primary cells by:

$$\forall \mathbf{x} \in K_{i,j}, \quad \tau_p(\mathbf{x}) = \frac{\eta_p}{\lambda} \mathbf{f}(\mathbf{c}_{i,j})(\mathbf{c}_{i,j} - \mathbf{I}_d).$$

Then we set:

$$\forall (i, j) \in \mathcal{S}^x, \quad -(\operatorname{div} \tau_p)_{i-\frac{1}{2},j}^x = \frac{1}{|K_{i-\frac{1}{2},j}^x|} \int_{\Omega} \tau_p : \nabla^{\mathcal{M}} \phi^{x,(i-\frac{1}{2},j)}. \quad (10)$$

An easy computation shows that this relation may be recast as a finite volume formulation, in the sense that the right-hand side may be seen as a sum over the faces of $K_{i-\frac{1}{2},j}^x$ of a discretization of the flux associated to $\operatorname{div} \tau_p$, *i.e.* the integral of the first component of $\tau_p \mathbf{n}_{K,\sigma}$. However, as usual when such a duality technique is used, the approximation of the tensor at the horizontal faces may seem strange: indeed, it is a convex combination of the unknown in the two neighbouring cells, but with coefficients which are not those which would be given by a linear interpolation.

4 Numerical tests

We compare the proposed scheme to results from the literature for the flow of an Oldroyd-B fluid in lid-driven cavity with a Weissenberg number equal to 1. The computational domain is $\Omega = (0, 1)^2$ and the velocity is prescribed on the whole boundary: $\mathbf{u} = (8x^2(1-x)^2(1 + \tanh(8t - 4)), 0)^t$ on $(0, 1) \times \{1\}$, $\mathbf{u} = 0$ otherwise. The fluid is initially at rest and the conformation tensor is set to identity. The computation is performed up to $t = 30$. The constant coefficients in System (1) are set to $\rho = 1$, $\eta_s = 0.5$, $\eta_p = 0.5$ and $\lambda = 1$. We use a sequence of successively refined meshes: the coarsest three ones are uniform 64×64 , 128×128 and 256×256 cells; the four other ones, denoted by Mn , $n = 1, \dots, 4$, use a uniform step equal to $1/(256n)$ in the x -direction and a splitting in the y -direction with a first step equal to $0.004/n$, a last step equal to $0.001/n$ and a constant ratio between two consecutive steps. The number of cells for the M4 mesh is close to 5.2 million. The sub-time-step for the solution of the ODE (3b) is set to $\delta t/n_e$ with n_e the smallest integer number such that $\delta t/n_e \leq 1/(2m \|\nabla_K \mathbf{u}^{n+1}\|_\infty)$, with $m = 10$ for the uniform meshes and $m = 200$ (to force convergence) for the Mn meshes; this time-step is small enough to preserve the positive definiteness of the conformation tensor when solving (3b) by a backward Euler scheme. Computations are run (in parallel for Meshes Mn) with the open-source CALIF³S software developed at IRSN [3]. The CPU-time used for the solution of the ODE remains almost negligible (less than 3% of the total time), so a more sophisticated algorithm would not enhance the scheme efficiency.

We first describe the results obtained with the three coarsest meshes, with a time-step equal to 0.01. In any case, computations reach a steady state. For the first component of the velocity along the line $x = 0.5$ (Figure 2, left), the steady state values are almost independent from the mesh, and in close agreement with those given in [8]. The convergence for the second component of the velocity along the line $y = 0.75$ (Figure 2, right) is a little bit slower: in the eyeball norm, convergence is

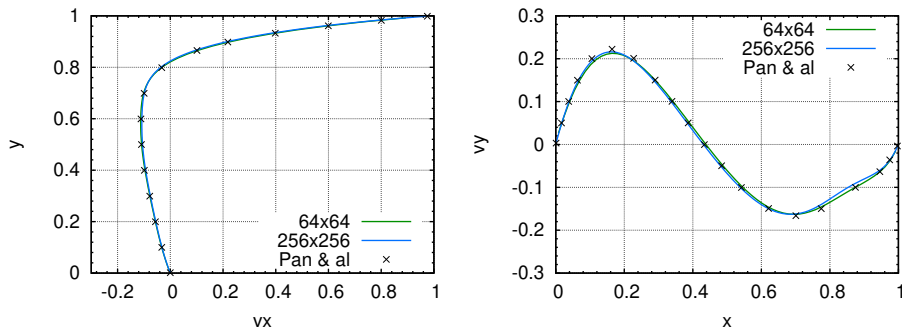


Fig. 2 Left: first component of the velocity along the line $x = 0.5$ – Right: second component of the velocity along the line $y = 0.75$.

obtained with the 256×256 mesh and the solution slightly differs from [8]. The most difficult point of this computation consists in obtaining an accurate estimation of the conformation tensor near the lid, and we investigate this issue with the M_n meshes. First of all, we observe that the time-step must be considerably reduced to obtain a stationary solution: $\delta t = 0.001$ for the $M1$, $M2$ and $M3$ meshes, and $\delta t = 0.0005$ for the $M4$ mesh. With a larger time-step, low-frequency instabilities (period in range of 1s) develop from the top-right corner, and remain confined in an area very close to the lid and included in the right half of the cavity. We plot in Figure 3 the computed value of c_{xx} along the lines $y = 0.975$ and $y = 1$. At $y = 0.975$, convergence seems to be almost achieved. The picture is completely different at $y = 1$: first, the profile of c_{xx} dramatically changes from $y = 0.975$; second, the maximum value, obtained close to $x = 0.5$, increases when refining the mesh (multiplication by a 1.6 factor when dividing the space step by 2 for $M2$, $M3$ and $M4$).

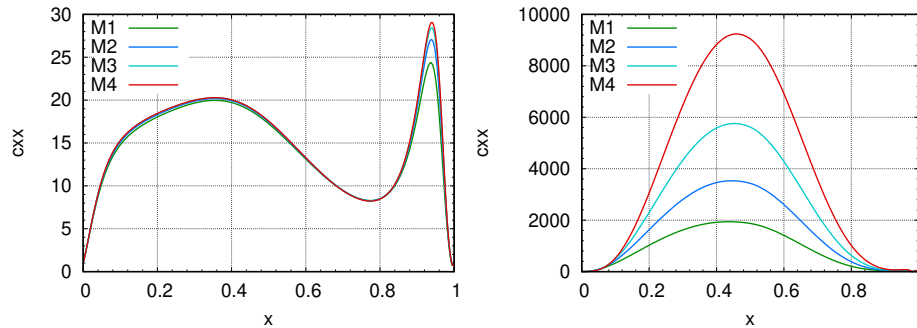


Fig. 3 Conformation tensor component c_{xx} along the line $y = 0.975$ (left) and $y = 1$ (right).

References

1. Bird, R.B., Wiest, J.M.: Constitutive Equations for Polymeric Liquids p. 25
2. Boyaval, S., Lelièvre, T., Mangoubi, C.: Free-energy-dissipative schemes for the Oldroyd-B model. *Mathematical Modelling and Numerical Analysis* **43**, 523–561 (2009)
3. CALIF³S: A software components library for the computation of fluid flows. <https://gforge.irsn.fr/gf/project/calif3s>
4. Fattal, R., Kupferman, R.: Time-dependent simulation of viscoelastic flows at high Weissenberg number using the log-conformation representation (2005)
5. Gallouët, T., Herbin, R., Latché, J.C., Mallem, K.: Convergence of the MAC scheme for the incompressible Navier-Stokes equations. *Foundations of Computational Mathematics* **18**(1), 249–289 (2018)
6. Grapsas, D., Herbin, R., Kheriji, W., Latché, J.C.: An unconditionally stable staggered pressure correction scheme for the compressible Navier-Stokes equations. *SMAI Journal of Computational Mathematics* **2**, 51–97 (2016)
7. Oishi, C., Martins, F., Tom, M., Cuminato, J., McKee, S.: Numerical solution of the extended pom-pom model for viscoelastic free surface flows. *Journal of Non-Newtonian Fluid Mechanics* **166**(3), 165 – 179 (2011)
8. Pan, T.W., Hao, J., Glowinski, R.: On the simulation of a time-dependent cavity flow of an Oldroyd-B fluid. *International Journal for Numerical Methods in Fluids* **60**, 791–808 (2009)